Journal of Engineering Physics and Thermophysics, Vol. 80, No. 5, 2007

NUMERICAL ANALYSIS OF THE PROCESS OF COMBUSTION AND GASIFICATION OF THE POLYDISPERSE COKE RESIDUE OF HIGH-ASH COAL UNDER PRESSURE IN A FLUIDIZED BED

A. Yu. Maistrenko,[a] V. P. Patskov,[a] A. I. Topal,[a] and T. V. Patskova[b]

UDC 662.04: 549.21

A numerical analysis of the process of "wet" gasification of high-ash coal under pressure in a low-temperature fluidized bed has been performed. The applicability of the previously developed computational model, algorithm, and program for the case under consideration has been noted. The presence of "hot spots" (short-time local heatings) at different points of the bed has been confirmed.

Introduction. In [1–5], we proposed a nonstationary mathematical model, an algorithm, and a program for calculating the process of combustion and gasification of the coke-ash residue of power coal in plants with a low-temperature fluidized bed. The development of such kinds of models, algorithms, and programs is an urgent and important problem both for developing methods of mathematical modeling, calculation, and optimization of the above class of processes and plants and for solving practical problems of creating systems for controlling the process, the temperature of the bed and the gas-distributing lattice, searching for slagless operational conditions of the bed, analyzing the transient processes including the start and stop of apparatuses, testing proposals and hypothesis advanced, optimizing the test conditions, and planning experiments in plants. The existing stationary mathematical models, algorithms, and programs [6, 7] do not permit complete solution of these problems.

The main goal of the investigation of [1–5] was to develop a methodology for calculating the processes of combustion and gasification of polydisperse coke residues of fuels in the zone of the fluidized bed of the reactor of the TsKS-1.0 pilot demonstration plant [8, 9] designed for thermochemical processing (pyrolysis, burning, gasification) of the high-ash Ukrainian coals in a circulating fluidized bed (CFB) at pressures up to 2.5 MPa and a high circulation ratio of the fuel (up to 100).

In [1–3], we made calculations on the influence of the pressure, the gas temperature, the fractional composition of the fuel, the mass consumption of coal, and the mass rate of flow of air on the proceeding of the process of combustion–gasification of the GSSh (gas-flame seedy culm) high-ash coal in the zone of the fluidized bed for the case of the so-called "dry" air gasification of the fuel [10]:

$$C + O_2 \rightarrow CO_2 , \tag{1}$$

$$C + 0.5O_2 \rightarrow CO , \tag{2}$$

$$C + CO_2 \rightarrow 2CO , \tag{3}$$

$$CO + 0.5O_2 \leftrightarrow CO_2 . \tag{4}$$

It has been established that the developed computational mathematical model, algorithm, and program are fairly effective and stable; they permit numerical analysis of both transient nonstationary and stationary temperature regimes of

[a]Institute of Coal Power Technologies, NAS of Ukraine, 19 Andreevskaya Str., Kiev, 04070; [b]National Technical University, Ukraine, Kiev; email:vadimpatskov@ukr.net. Translated from Inzhenerno-Fizicheskii Zhurnal, Vol. 80, No. 5, pp. 160–171, September–October, 2007. Original article submitted July 20, 2005; revision submitted March 12, 2007.

1062-0125/07/8005-1019

the process in a wide range of regime parameters and physicochemical and structural characteristics of the fuel, attaining in the course of calculations effective times and degrees of transformation of the fuel comparable to those observed in the pilot and pilot-industrial plants [8, 9]. We have revealed the presence of so-called "hot spots" (short-time local heatings) at different points of the bed associated with the disturbance of balances in the nonstationary transient regimes between the heat release as a result of homogeneous and heterogeneous chemical transformations and the heat input due to the convective, radiative, and interphase heat exchange. We also noted the possibility of using the mathematical model to predict and eliminate the above effects.

Formulation of the Problem. In the present paper, we consider the case of the so-called "wet" gasification [10] of solid fuel in a fluidized bed characterized, apart from reactions (1)–(4), by the following chemical transformations [4, 10]:

$$C + H_2O \rightarrow CO + H_2 , \tag{5}$$

$$C + 2H_2 \rightarrow CH_4 , \tag{6}$$

$$CO + H_2O \leftrightarrow CO_2 + H_2 , \tag{7}$$

$$CO + 3H_2 \rightarrow CH_4 + H_2O , \tag{8}$$

$$CO_2 + 4H_2 \rightarrow CH_4 + 2H_2O , \tag{9}$$

$$H_2 + 0.5O_2 \leftrightarrow H_2O , \tag{10}$$

$$CH_4 + 2O_2 \rightarrow CO_2 + 2H_2O . \tag{11}$$

In constructing the mathematical description of the process, the following assumptions are made [1–5]:

1. The fluidized bed zone includes the following phases: a) the dense phase containing solid particles of the coke-ash residue of the fuel and ash, as well as the gas flowing between them and needed for the onset of fluidization; b) the bubble phase representing the gas bypassing between the particles, with bubbles changing size as they move on the bed.

2. The transfer processes in the bubble phase proceed in the regime of perfect displacement, and for their description in the dense phase one uses a model taking into account the effective diffusion and the heat conductivity, as well as the filtration of the components in the bed in order to reflect the deviations from the perfect mixing regime caused by the circulation of solid particles, the transfer of a portion of the gas with moving bubbles, the heat and mass transfer between the bubbles and the gas flow in the dense phase, and the mixing mechanism analogous to the Taylor diffusion and associated with the presence of size dispersion of the bubbles [11].

3. To analyze the qualitative mechanisms of transformations of solid fuel particles in the bed at relatively short times corresponding to the transient regimes of combustion and gasification of power coals in a fluidized bed, it is recommended [11] to use the diffusion model taking into account the effective coefficients of longitudinal mixing and the circulation velocity of the solid particles.

4. In the dense phase, the surface heterogeneous reactions of combustion and gasification of the coke-ash residue (1)–(3), (5), (6), as well as a homogeneous reaction of CO oxidation (4) proceed.

5. In the bubble phase, solid particles are absent and the homogeneous chemical reactions (4) and (7)–(11) proceed.

6. The initial fractional composition of the coke fed into the apparatus is described by the Rosin–Rammler size distribution function [6, 7, 12].

7. The coke fuel particles are spherical. We take the AS-model of the thermochemical transformation of fuel particles as the ash falls off from their outer surface, which is due to the intensive mixing of solid particles in the bed, their collision, breaking, and other interaction effects [6, 7].

Mathematical Model of the Process. On the basis of the assumptions made, the system of equations of the model in the nonstationary one-dimensional formulation is of the form [5]

Dense phase of the bed

$$\varepsilon^{\mathrm{d}}\rho_1^{\mathrm{d}}\frac{\partial C_j^{\mathrm{d}}}{\partial t}=D_j^{\mathrm{d}}\frac{\partial}{\partial x}\left[\varepsilon^{\mathrm{d}}\rho_1^{\mathrm{d}}\frac{\partial C_j^{\mathrm{d}}}{\partial x}\right]-u_1^{\mathrm{d}}\varepsilon^{\mathrm{d}}\rho_1^{\mathrm{d}}\frac{\partial C_j^{\mathrm{d}}}{\partial x}-\mathrm{K}_{\mathrm{b.e}}\left(\rho_j^{\mathrm{d}}-\rho_j^{\mathrm{b}}\right)+\int_{r_0^{\mathrm{c}}}^{r^{\mathrm{c}}}\nu_{s,j}W_sF_{\mathrm{sp}}^{\mathrm{c}}f_l^{\mathrm{c}}(r)\,dr+$$

$$+\sum_{q=1}^{n_q}\nu_{qj}W_q\,,\quad j=\overline{1,m_{\mathrm{gas}}}\,,\quad q=\overline{1,n_q}\,; \tag{12}$$

$$\varepsilon^{\mathrm{d}}\rho_1^{\mathrm{d}}c_{p1}^{\mathrm{d}}\frac{\partial T_1^{\mathrm{d}}}{\partial t}=\lambda_1^{\mathrm{d}}\frac{\partial^2 T_1^{\mathrm{d}}}{\partial x^2}-u_1^{\mathrm{d}}\rho_1^{\mathrm{d}}c_{p1}^{\mathrm{d}}\varepsilon^{\mathrm{d}}\frac{\partial T_1^{\mathrm{d}}}{\partial x}-$$

$$-\mathrm{H}_{\mathrm{b.e}}\left(T_1^{\mathrm{d}}-T_1^{\mathrm{b}}\right)-\int_{r_0^{\mathrm{c}}}^{r^{\mathrm{c}}}\left\{\mathrm{H}_{\mathrm{conv}}^{\mathrm{c}}\left(T_1^{\mathrm{d}}-T_l^{\mathrm{c}}\right)+\varphi^{\mathrm{c}}\sigma_0\kappa^{\mathrm{c}}\left[\left(\frac{T_1^{\mathrm{d}}}{100}\right)^4-\left(\frac{T_l^{\mathrm{c}}}{100}\right)^4\right]\right\}F_{\mathrm{sp}}^{\mathrm{c}}f_l^{\mathrm{c}}(r)\,dr-\mathrm{H}_{\mathrm{w}}\left(T_1^{\mathrm{d}}-T_{\mathrm{w}}\right)+$$

$$+\sum_{q=1}^{n_q}W_qQ_q+\int_{r_0^{\mathrm{a}}}^{r^{\mathrm{a}}}\left\{\mathrm{H}_{\mathrm{conv}}^{\mathrm{a}}\left(T_1^{\mathrm{d}}-T_l^{\mathrm{a}}\right)+\varphi^{\mathrm{a}}\sigma_0\kappa^{\mathrm{a}}\left[\left(\frac{T_1^{\mathrm{d}}}{100}\right)^4-\left(\frac{T_l^{\mathrm{a}}}{100}\right)^4\right]\right\}F_{\mathrm{sp}}^{\mathrm{a}}f_l^{\mathrm{a}}(r)\,dr\,,\quad l=\overline{1,N^{\mathrm{sort}}}\,,\quad \mathrm{sort}=\mathrm{c},\,\mathrm{a}\,, \tag{13}$$

$$t=0\,,\quad x=0:\quad C_j^{\mathrm{d}}=C_{0j}^0\quad (j=1,\ldots,m_{\mathrm{gas}})\,,\quad T_1^{\mathrm{d}}=T_{0,1}\,, \tag{14}$$

$$x=L_{\mathrm{bed}}:\quad \frac{\partial C_j^{\mathrm{d}}}{\partial x}=\frac{\partial T_1^{\mathrm{d}}}{\partial x}=0\,. \tag{15}$$

The first term on the right-hand side of Eq. (12) represents the mass transfer of the jth gaseous component in the dense phase due to the longitudinal effective diffusion, the second term — the convective-filtration transfer, the third one — the interphase mass transfer between the dense phase and the bubbles, and the fourth one — the convective mass transfer between the gas flow in the dense phase and the surface of the fuel particles. The first term on the right-hand side of Eq. (13) corresponds to the energy transfer in the dense phase due to the effective parallel thermal conductivity, the second one corresponds to the convective-filtration transfer, the third one — to the interphase heat transfer between the dense and bubble phases, the fourth one — to the convective and radiative heat transfer between the coke-ash fractions and the gas flow in the dense phase, the fifth one — to the near-wall heat transfer, the sixth one — to the heat release due to the homogeneous chemical transformations, and the seventh one — to the convective and radiative heat transfer between the ash fractions and the gas flow in the dense phase.

The bubble phase is

$$u_*^{\mathrm{b}}\alpha_*^{\mathrm{b}}\rho_1^{\mathrm{b}}\frac{\partial C_j^{\mathrm{b}}}{\partial x}+\alpha_*^{\mathrm{b}}\rho_1^{\mathrm{b}}\frac{\partial C_j^{\mathrm{b}}}{\partial t}=\sum_{q=1}^{n_q}\nu_{qj}W_q+\mathrm{K}_{\mathrm{b.e}}\left(\rho_j^{\mathrm{b}}-\rho_j^{\mathrm{d}}\right),\quad j=\overline{1,m_{\mathrm{gas}}}\,; \tag{16}$$

$$u_*^{\mathrm{b}}\alpha_*^{\mathrm{b}}\rho_1^{\mathrm{b}}c_{p1}^{\mathrm{b}}\frac{\partial T_1^{\mathrm{b}}}{\partial x}+\alpha_*^{\mathrm{b}}\rho_1^{\mathrm{b}}c_{p1}^{\mathrm{b}}\frac{\partial T_1^{\mathrm{b}}}{\partial t}=\sum_{q=1}^{n_q}W_qQ_q+\mathrm{H}_{\mathrm{b.e}}\left(T_1^{\mathrm{b}}-T_1^{\mathrm{d}}\right); \tag{17}$$

$$t=0\,,\quad x=0:\quad C_j^{\mathrm{b}}=C_{0j}\quad (j=1,\ldots,m_{\mathrm{gas}})\,,\quad T_1^{\mathrm{b}}=T_{0,1}\,. \tag{18}$$

The first terms on the right sides of Eqs. (16) and (17) present the change in the mass of the *j*th gaseous component and the heat release as a result of the homogeneous chemical reactions, the second ones — the interphase mass and heat transfer between the bubbles and the dense phase of the bed.

The size distribution of particles is

$$D_l^{\mathrm{c}}\frac{\partial^2 f_l^{\mathrm{c}}}{\partial x^2}\pm u_l^{\mathrm{c}}\frac{\partial f_l^{\mathrm{c}}}{\partial x}-\frac{\partial}{\partial r}\left\{\frac{f_l^{\mathrm{c}}}{\rho_2^{\mathrm{c}}}\left[\sum_{s=1}^{n_s}\nu_s^{\mathrm{c}}W_s+C_l^{\mathrm{c}}K_{\mathrm{car}}^{\mathrm{c}}\right]\right\}=\frac{\partial f_l^{\mathrm{c}}}{\partial t}\,,\quad l=\overline{1,N^{\mathrm{c}}}\,; \tag{19}$$

$$D_l^{\mathrm{a}}\frac{\partial^2 f_l^{\mathrm{a}}}{\partial x^2}\pm u_l^{\mathrm{a}}\frac{\partial f_l^{\mathrm{a}}}{\partial x}-\frac{\partial}{\partial r}\left[\frac{f_l^{\mathrm{a}}}{\rho_2^{\mathrm{a}}}\left\{C_l^{\mathrm{a}}K_{\mathrm{car}}^{\mathrm{a}}\right\}\right]=\frac{\partial f_l^{\mathrm{a}}}{\partial t}\,,\quad l=\overline{1,N^{\mathrm{a}}}\,; \tag{20}$$

$$t=0:\quad f_l^{\mathrm{sort}}=f_{0l}=f_l^{\mathrm{p}}\,; \tag{21}$$

$$x=0:\quad D_l^{\mathrm{sort}}\frac{\partial f_l^{\mathrm{sort}}(r)}{\partial x}=u_l^{\mathrm{p}}f_l^{\mathrm{p}}(r)-u_l^{\mathrm{sort}}f_l^{\mathrm{sort}}(r)\,,\quad l=\overline{1,N^{\mathrm{sort}}}\,; \tag{22}$$

$$x=L_{\mathrm{bed}}:\quad D_l^{\mathrm{sort}}\frac{\partial f_l^{\mathrm{sort}}(r)}{\partial x}=u_{\mathrm{hov}}f_l^{\mathrm{sort}}(r)\quad \left(u_l^{\mathrm{sort}}\ge u_{\mathrm{hov}}\right)\quad D_l^{\mathrm{sort}}\frac{\partial f_l^{\mathrm{sort}}(r)}{\partial x}=0\quad \left(u_l^{\mathrm{sort}}<u_{\mathrm{hov}}\right). \tag{23}$$

The first term on the left side of Eq. (19) presents the change in the portion of coke-ash fractions in terms of the longitudinal effective diffusion, the second one — the convective heat transfer due to the circulation of particles, the third one — the expenditure of particles due to the heterogeneous chemical transformations and carry-over. In Eq. (20) describing the change in the portion of ash fractions, the physical meaning of the first two terms on the left side is analogous to (19), and the third one — to the carry-over.

Individual particles of the coke-ash residue and ash

$$\rho_1^{\mathrm{surf}}\frac{\partial C_j^{\mathrm{surf}}}{\partial t}=\left[\beta_j\left(\rho_j^{\mathrm{surf}}-\rho_j^{\mathrm{d}}\right)+\nu_s^{\mathrm{c}}W_s\right]\left(1-\varepsilon_{\mathrm{f}}\right)F_{\mathrm{sp}}^{\mathrm{c}}\left(1-\varepsilon^{\mathrm{d}}\right)\left(1-\alpha_*^{\mathrm{b}}\right),\quad j=\overline{1,m_{\mathrm{gas}}}\,; \tag{24}$$

$$\rho_2^{\mathrm{c}}c_{p2}^{\mathrm{c}}\frac{\partial T_l^{\mathrm{c}}}{\partial t}=\left\{\sum_{s=1}^{n_s}W_sQ_s+\mathrm{H}_{\mathrm{conv}}^{\mathrm{c}}\left(T_1^{\mathrm{d}}-T_l^{\mathrm{c}}\right)+\kappa^{\mathrm{c}}\sigma_0\left[\left(\frac{T_1^{\mathrm{d}}}{100}\right)^4-\left(\frac{T_l^{\mathrm{c}}}{100}\right)^4\right]\right\}\left(1-\varepsilon_{\mathrm{f}}\right)F_{\mathrm{sp}}^{\mathrm{c}}\left(1-\varepsilon^{\mathrm{d}}\right)\left(1-\alpha_*^{\mathrm{b}}\right), \tag{25}$$

$$l=\overline{1,N^{\mathrm{c}}}\,;$$

$$\rho_2^{\mathrm{a}}c_{p2}^{\mathrm{a}}\frac{\partial T_l^{\mathrm{a}}}{\partial t}=\left\{\mathrm{H}_{\mathrm{conv}}^{\mathrm{a}}\left(T_1^{\mathrm{d}}-T_l^{\mathrm{a}}\right)+\kappa^{\mathrm{a}}\sigma_0\left[\left(\frac{T_1^{\mathrm{d}}}{100}\right)^4-\left(\frac{T_l^{\mathrm{a}}}{100}\right)^4\right]\right\}\left(1-\varepsilon_{\mathrm{f}}\right)F_{\mathrm{sp}}^{\mathrm{a}}\left(1-\varepsilon^{\mathrm{d}}\right)\left(1-\alpha_*^{\mathrm{b}}\right),\quad l=\overline{1,N^{\mathrm{a}}}\,; \tag{26}$$

$$t = 0: \quad C_j^{\text{surf}} = C_{0j} \quad (j = 1, ..., m_{\text{gas}}), \quad T_l^{\text{c}} = T_l^{\text{a}} = T_{0,2} \quad (l = 1, ..., N^{\text{sort}}). \tag{27}$$

Equation (24) defines the change in the surface concentration of the *j*th gaseous component due to the convective mass transfer between the gas flow in the dense phase and the surface of fuel particles and the heterogeneous chemical transformations. Equation (25) defines the change in the surface temperature of the coke-ash fractions due to the heat release caused by the surface chemical transformations and the convective and radiative heat transfer between the phases. Equation (26) corresponds to the change in the temperatures of ash particles due to the convective and radiative heat transfer between the gas flow in the dense phase and the particle surface.

The equations of state and normalization condition are

$$P_{0,1} = \rho_1^i R T_1^i \sum_{j=1}^{m_{\text{gas}}} \frac{C_j^i}{M_j}, \quad j = \overline{1, m_{\text{gas}}}, \quad i = \text{d, b}; \tag{28}$$

$$\sum_{j=1}^{m_{\text{gas}}} C_j^i = 1, \quad \alpha_*^{\text{b}} + \varepsilon^{\text{d}} = 1; \tag{29}$$

$$u_1^{\text{d}} = u_{\text{mf}} / \varepsilon_{\text{mf}} = u_0 / \varepsilon^{\text{d}}. \tag{30}$$

The energy transfer in the reactor walls is [13]

$$\frac{\partial T_{\text{w}}}{\partial t} = a_{\text{w}} \frac{\partial^2 T_{\text{w}}}{\partial x^2}, \tag{31}$$

$$T_{\text{w}}(0, t) = T_{0\text{w}}, \tag{32}$$

$$T_{\text{w}}(L_{\text{bed}}, t) = \overline{T}^* = \text{const}, \tag{33}$$

$$T_{\text{w}}(x, 0) = T_{\text{w}}(0) + \frac{\overline{T}^* - T_{\text{w}}(0)}{\delta_{\text{w}}} x. \tag{34}$$

Determination of the main parameters of the model. The porosity and the working height of the fluidized bed are estimated on the basis of the law of expansion of the homogeneous fluidized bed [11]

$$\varepsilon = \varepsilon_{\text{mf}} \left[\frac{\text{Re} + 0.02\text{Re}^2}{\text{Re}_{\text{mf}} + 0.02\text{Re}_{\text{mf}}^2} \right]^{0.1}, \quad L_{\text{bed}} = L_0 \frac{1 - \varepsilon_{\text{mf}}}{1 - \varepsilon},$$

where

$$\text{Re} = \frac{u_0 \overline{d}_{\text{part}}^{\text{eqv}}}{\eta_1}; \quad \text{Re}_{\text{mf}} = \frac{u_{\text{mf}} \overline{d}_{\text{part}}^{\text{eqv}}}{\eta_1}; \quad \overline{d}_{\text{part}}^{\text{eqv}} = \sum_{l=1}^{N^{\text{c}}+N^{\text{a}}} \frac{\overline{\psi}_l^{\text{sort}}}{\overline{d}_l^{\text{sort}}}.$$

The minimum velocities of onset of fluidization and hovering are estimated by the known criteria formulas [11]

$$\mathrm{Re}_{\mathrm{mf}} = \frac{\mathrm{Ar}}{1400 + 5.22\sqrt{\mathrm{Ar}}}, \quad \mathrm{Re}_{\mathrm{hov}} = \frac{u_{\mathrm{hov}} \bar{d}_{\mathrm{part}}^{\,\mathrm{eqv}}}{\eta_1} = \frac{\mathrm{Ar}\varepsilon^{4.75}}{18 + 0.61\sqrt{\mathrm{Ar}\varepsilon^{4.75}}}. \tag{35}$$

The effective diffusion coefficients in the gas phase are taken equal to the diffusion coefficients of the corresponding components.

The coefficients of interphase heat and mass transfer between the dense and bubble phases are estimated by the relations of the Kunin–Levenspiel model [14]

$$\frac{1}{\mathrm{K}_{\mathrm{b.e}}} = \frac{1}{\mathrm{K}_{\mathrm{c.e}}} + \frac{1}{\mathrm{K}_{\mathrm{b.c}}}, \quad j = \overline{1, m_{\mathrm{gas}}}; \quad \mathrm{K}_{\mathrm{b.c}} = 4.5\left(\frac{\varepsilon_{\mathrm{mf}} u_{\mathrm{mf}}}{d^{\mathrm{b}}}\right) + 5.85\left(\frac{D_j g^{0.5}}{(\bar{d}^{\,\mathrm{b}})^{5/4}}\right); \quad \mathrm{K}_{\mathrm{c.e}} = 6.78\left(\frac{\varepsilon_{\mathrm{mf}} D_j u_*^{\mathrm{b}}}{(\bar{d}^{\,\mathrm{b}})^3}\right);$$

$$\frac{1}{\mathrm{H}_{\mathrm{b.e}}} = \frac{1}{\mathrm{H}_{\mathrm{c.e}}} + \frac{1}{\mathrm{H}_{\mathrm{b.c}}}; \quad \mathrm{H}_{\mathrm{b.c}} = 4.5\left(\frac{\varepsilon_{\mathrm{mf}} u_{\mathrm{mf}} \rho_1^{\mathrm{d}} c_{p1}^{\mathrm{d}}}{\bar{d}^{\,\mathrm{b}}}\right) + 10.4\left(\frac{\lambda_1^{\mathrm{d}} c_{p1}^{\mathrm{d}} \rho_1^{\mathrm{d}}}{(\bar{d}^{\,\mathrm{b}})^{5/4}}\right);$$

$$\mathrm{H}_{\mathrm{c.e}} = 6.78\,\lambda_1^{\mathrm{d}} c_{\mathrm{p1}}^{\mathrm{d}} \rho_1^{\mathrm{d}}\left(\frac{\varepsilon_{\mathrm{mf}} u_*^{\mathrm{b}}}{(\bar{d}^{\,\mathrm{b}})^3}\right)^{1/2}.$$

To calculate the bubble diameter averaged over the bed cross-section, we use the relations [7, 15]

$$\bar{d}^{\,\mathrm{b}} = 0.16\,(u_0 - u_{\mathrm{mf}})^{0.55}\,(x + x_0),$$

where x_0 is a constant corresponding to the initial diameter of bubbles formally equal to

$$x_0 = \frac{\bar{d}_0^{\,\mathrm{b}}}{\left[0.16\,(u_0 - u_{\mathrm{mf}})^{0.55}\right]^{4/3}};$$

$\bar{d}_0^{\,\mathrm{b}}$ is the initial diameter of bubbles calculated by the formula

$$\bar{d}_0^{\,\mathrm{b}} = 0.00376\,(u_0 - u_{\mathrm{mf}})^2.$$

The local velocities of emersion of bubbles in the bed are estimated by the relations [10, 11, 15, 16]

$$u_*^{\mathrm{b}} = u_0 - \left(1 - \alpha_*^{\mathrm{b}}\right) u_{\mathrm{mf}} \varepsilon_{\mathrm{mf}} + 0.71\sqrt{g\bar{d}^{\,\mathrm{b}}} \quad \left(\frac{\bar{d}^{\,\mathrm{b}}}{d_{\mathrm{ap}}} < 0.5\right),$$

$$u_*^{\mathrm{b}} = u_0 - \left(1 - \alpha_*^{\mathrm{b}}\right) u_{\mathrm{mf}} \varepsilon_{\mathrm{mf}} + 0.35\sqrt{g\bar{d}^{\,\mathrm{b}}} \quad \left(\frac{\bar{d}^{\,\mathrm{b}}}{d_{\mathrm{ap}}} \geq 0.5\right).$$

The rates of surface heterogeneous reactions of coke combustion (1) and (2) are determined by the relations [9]

$$W_1 = \chi k_1^0 \exp\left[(E_1/R)\,(1/T_0^{\mathrm{c}} - 1/T_l^{\mathrm{c}})\right] C_{\mathrm{O}_2}^{\mathrm{F}}\,(C_{\mathrm{O}_2} T_0^{\mathrm{c}} / C_{\mathrm{O}_2}^{\mathrm{F}} T_l^{\mathrm{c}})^{\gamma}, \quad l = 1, \ldots, N^{\mathrm{c}};$$

$$W_2 = (1 - \chi)\,k_2^0 \exp\left[(E_2/R)\,(1/T_0^{\mathrm{c}} - 1/T_l^{\mathrm{c}})\right] C_{\mathrm{O}_2}^{\mathrm{F}}\,(C_{\mathrm{O}_2} T_0^{\mathrm{c}} / C_{\mathrm{O}_2}^{\mathrm{F}} T_l^{\mathrm{c}})^{\gamma},$$

where $\chi = 0.45$ for the intradiffusion and $\chi = 0.465$ for the transient regimes of reaction between the kinetic and the intradiffusion regimes is the generalized stoichiometric coefficient; k_s^0 (s = 1, 2) denotes the reaction rate constants at

the reference temperature T_0^c; $E_{1,2}$ stands for the observed activation energies; $\gamma = 0.85$ for the intradiffusion and $\gamma = 1$ for the transient regimes of reaction; $C_{0,2}^F$ is the fixed concentration of O_2 under normal conditions.

The rate of the heterogeneous reaction of coke gasification (3) with CO_2 is determined by an equation analogous to the Langmuir–Hinshelwood model [9, 17]:

$$W_3 = \frac{k_3^0 \exp\left[\frac{E_1}{R}\left(\frac{1}{T_0^c} - \frac{1}{T_l^c}\right)\right] p_{CO_2}}{1 + k_4^0 \exp\left[\frac{E_2}{R}\left(\frac{1}{T_l^c} - \frac{1}{T_0^c}\right)\right] p_{CO_2} + k_5^0 \exp\left[\frac{E_3}{R}\left(\frac{1}{T_l^c} - \frac{1}{T_0^c}\right)\right] p_{CO}}, \quad l = \overline{1, N^c}.$$

The reaction rate of steam gasification of coke (5) is calculated similarly to the expression [18, 19]

$$W_5 = \frac{k_6^0 \exp\left[\frac{E_4}{R}\left(\frac{1}{T_0^c} - \frac{1}{T_l^c}\right)\right] p_{H_2O}}{1 + k_7^0 \exp\left[\frac{E_5}{R}\left(\frac{1}{T_l^c} - \frac{1}{T_0^c}\right)\right] p_{H_2O} + k_8^0 \exp\left[\frac{E_6}{R}\left(\frac{1}{T_l^c} - \frac{1}{T_0^c}\right)\right] p_{H_2}}, \quad l = \overline{1, N^c}.$$

The hydrogasification rate of coke (6) is determined by the equation [18]

$$W_6 = k_9^0 \exp\left[\frac{E_9}{R}\left(\frac{1}{T_0^c} - \frac{1}{T_l^c}\right)\right] p_{H_2}, \quad l = \overline{1, N_l^c}.$$

The rate of the homogeneous reaction (4) of CO oxidation is taken from [20]

$$W_4 = k_{10}^0 \exp\left[\frac{E_{10}}{R}\left(\frac{1}{T_{0,1}} - \frac{1}{T_1^i}\right)\right] \rho_{CO} \rho_{O_2}^{0.5} \rho_{H_2}^{0.5} - k_{11}^0 \exp\left[\frac{E_{11}}{R}\left(\frac{1}{T_{0,1}} - \frac{1}{T_1^i}\right)\right] \rho_{CO_2}, \quad i = \text{b, d}.$$

To calculate the rates of the homogeneous "water displacement" reaction (7), we use the expressions [21]

$$W_7 = k_{12}^0 \exp\left[\frac{E_{12}}{R}\left(\frac{1}{T_{0,1}} - \frac{1}{T_1^i}\right)\right] \rho_{CO} \rho_{H_2O} - k_{13}^0 \exp\left[\frac{E_{13}}{R}\left(\frac{1}{T_{0,1}} - \frac{1}{T_1^i}\right)\right] \rho_{CO_2} \rho_{H_2}.$$

To calculate the rates of the methane conversion reactions (8) and (9), we use the equations [22]

$$W_{8,9} = \frac{k_{14,15}^0 y_k \exp\left[\vartheta\left(1 - \frac{T_1^i}{T_{0,1}}\right)\right]}{\left[1 + k_{16,17}^0 y_k \exp\left[\vartheta_n\left(1 - \frac{T_1^i}{T_{0,1}}\right)\right]\right]^{\upsilon}}. \tag{36}$$

The rate of the homogeneous reaction of hydrogen oxidation (10) is calculated as [20, 21]

$$W_{10} = k_{18}^0 \exp\left[\frac{E_{18}}{R}\left(\frac{1}{T_{0,1}} - \frac{1}{T_1^i}\right)\right] \rho_{H_2}^2 \rho_{O_2} / \rho_{CO}.$$

The rate of the homogeneous reaction of methane combustion (11) is calculated according to the relation [23]

TABLE 1. Calculation Formulas Used to Estimate the Heat and Mass Transfer Coefficients

Heat transfer	Mass transfer	Aplication conditions	Literature source
$Nu = Nu_{max} + (Nu_1 - Nu_{max}) \times \times \exp\left[-\frac{d^c_{part}}{4d^a_{part}}\right]$	$Sh_1 = \frac{d^a_{part}}{d^c_{part}} + 0.009Ar_a^{0.5} \times \times \left[1 + (30Ar_a^{-1/6} - 1) \exp\left[-\frac{d^c_{part}}{4d^a_{part}}\right]\right]$	$d^c_{part} = d^a_{part} = (10—60)$ mm $Đ_{0,1} = 0.05—10$ MPa, $Ar = 10^2—10^7$	[16]
$Nu_{max} = 0.85Ar_a^{0.19} + 0.006\times \times Ar_a^{0.5} Pr_1^{0.333}$ $Nu_{a\infty} = 0.85Ar_a^{0.19} + 0.006\times \times Ar_a^{0.5} Pr_1^{0.333}$ $Nu_c = \left[(Nu_1 - Nu_{a\infty})\left(\frac{d^c_{part}}{d^a_{part}}\right)^{1/3} + Nu_{a\infty}\frac{d^c_{part}}{d^a_{part}}\right]\xi^{2/3}$	$Sh_{a\infty} = 0.009Ar_a^{0.5} Sc_1^{0.33}$ $Sh_c = (Sh_1 - Sh_{a\infty})\left(\frac{d^c_{part}}{d^a_{part}}\right)^{1/3} + +Sh_{a\infty}\frac{d^c_{part}}{d^a_{part}}$	$d^c_{part} >> d^a_{part}$ $d^a_{part} = 0.13—2.15$ mm $\rho^a_2 = 2300—3000$ kg/m^3 $Ar_a = 40—10^5$ $d^c_{part} = 5.3—36.8$ mm $\rho^a_2 = 1150—2700$ kg/m^3 (heat-transfer) $d^c_{part} = 2.4—21.9$ mm $\rho^c_2 = 820—2340$ kg/m^3 (mass-transfer)	[25]
$Nu_1 = 6.0 + 0.117Ar_a^{0.39} Pr_1^{0.333}$	$Sh_1 = 2\varepsilon_{mf} + 0.117Ar_a^{0.39} Sc_1^{0.333}$	$0.05 \le d^c_{part} \le 1.0$, $40 \le Ar_a \le 10^5$	[25]
$Nu_c = 2 + 0.6(Re^{eff})^{0.5}Pr_1^{0.333}$	$Sh_c = 2 + 0.6(Re^{eff})^{0.5}Sc_1^{0.333}$	$d^c_{part} = d^a_{part}$ $d^c_{part} << d^a_{part}$ $1 \le \frac{d^c_{part}}{d^a_{part}} \le \left(\frac{d^c_{part}}{d^a_{part}}\right)_{cr}$ $r = 0.7$; $10 \le Ar_a \le 10^5$	[25]
$Nu_1 = 10 + 0.23(Ar_aPr_1)^{0.333}$ $Nu_c = Nu_1\left(\frac{d^c_{part}}{d^a_{part}}\right)^r$	$Sh_c = Sh_1\left(\frac{d^c_{part}}{d^a_{part}}\right)^z$	$r = 0.39Ar_a^{0.105}$ $10^5 \le Ar_a \le 10^7$, $\exp(z) = 0.58Ar_c^{0.07}$, $10 \le Ar_c \le 150$ $\exp(z) = 0.509Ar_c^{0.1}$, $150 \le Ar_c \le 10^7$ $\left(\frac{d^c_{part}}{d^a_{part}}\right)_{cr} = 5.35\cdot Ar_a^{0.1}$, $10 \le Ar_a \le 5\cdot10^4$ $\left(\frac{d^c_{part}}{d^a_{part}}\right)_{cr} = 2.8Ar_c^{0.81}$, $5.0\cdot10^4 \le Ar_c \le 3.0\cdot10^8$	[25]

$$W_{11} = k^0_{19} \exp\left[\frac{E_{19}}{R}\left(\frac{1}{T_{0,1}} - \frac{1}{T^i_1}\right)\right] \rho_{CO} \rho^{0.25}_{O_2} \rho^{0.5}_{H_2O} \cdot$$

The thermal effects of reactions (1)–(12) depending on the ambient temperature are determined by the approximation polynomials of [24]. The effective longitudinal heat conductivity coefficients in the bed are estimated on

the basis of the recommendations given in [11, 16]. The heat transfer coefficients from the wall to the bed are determined by the relations [16]

$$H_w \approx 0.8 H_{max} ,$$

where H_{max} is the maximum heat transfer coefficient calculated by the relation [16]

$$Nu_{max} = 0.85 Ar_1^{0.19} + 0.006 Ar_1^{0.5} Pr_1^{0.33} .$$

The coefficients of convective heat and mass transfer between the active surface of the fuel particle and the surrounding gas are calculated on the basis of the criteria relations of [16, 25] taking into account the presence of inertial ash particles in the fluidized bed (see Table 1). The effective longitudinal transfer coefficient in the bed is determined by the relations [11, 16]

$$D_l^{sort} = \frac{1}{60} \sqrt{L_{bed}^2 g} .$$

The rate constants of the particle carry-over into the superbed space are estimated by the empirical Merrick and Hailey correlation [6, 7, 26]

$$K_{car}(r) \approx \frac{G_{car} f_{car}(r)}{\overline{\psi}^{sort} \Psi_{bed} f_l^{sort}(r)} \approx 130 \frac{\rho_1^d u_0 F_{an}}{\Psi_{bed}} \exp\left[-10.4 \left(\frac{u_{hov}}{u_0} \right)^{0.5} \left(\frac{u_{mf}}{u_0 - u_{mf}} \right)^{0.5} \right] .$$

Computational algorithm. In the numerical analysis of the problem, we calculate sequentially the process characteristics in the bubble phase, the surface concentrations of reagents, the surface temperature of the fuel and ash particles, the size distribution functions of solid fractions, and the process characteristics in the dense phase of the bed. In so doing, the systems of equations of transfer in the bubble phase (16)–(18) and on individual particles (24)–(27) are solved by the relaxation method of [27].

The transfer equations in the dense phase (12)–(15) and the equations for the size distribution functions of solid particles (19)–(23) and wall temperatures (31)–(34) are solved by the sweep method [28, 29]. In so doing, the integrals in Eqs. (12) and (13) are calculated by the Simpson method, and the source terms in Eqs. (19) and (20) are calculated by means of numerical differentiation [30]. In all thermal balance equations (13), (17), (25), and (26), temperature linearization of the terms taking into account the heat release due to the chemical transformations is realized.

A specific feature of the algorithm is automatic selection of the time step by means of Richardson extrapolation [28], in which a comparison of the maximal relative computational errors of the gas temperatures in the dense and bubble phases and of the integral mean temperatures of the coke-ash residue and ash at the whole time step and at two half-steps is made.

The computing program was developed in FORTRAN-90. The basic initial data for the calculations are: fractional portions of the fuel and ash, thermophysical characteristics of the fuel, ash, and gaseous components, data of the technical and elemental analysis of the coal, coke-ash residue, and ash, physical sizes of the apparatus, pressure, mass flow of air and coal consumption, initial temperatures of the coal, gases, ash, and walls, composition of the blow gases, and macrokinetic parameters of the chemical reactions.

The main results of the calculations are: fields of the main calculated variables in the phases of the bed on its height at different instants of time, size distribution functions of solid particles, degrees of conversion and sizes of particles, characteristics of the onset of fluidization and carry-over, mass-mean temperatures of the phases, walls, and bed, interphase heat and mass transfer coefficients, reaction rates, and parallel effective thermal conductivity of the bed.

Results of the Calculations and Discussion. In the numerical analysis of the model (12)–(33), we investigated the ignition dynamics of the fluidized bed in the process of thermochemical processing of high-ash coal. We varied the pressure, the initial temperatures of the fuel, ash, and gas, the fractional composition of the fuel, the mass

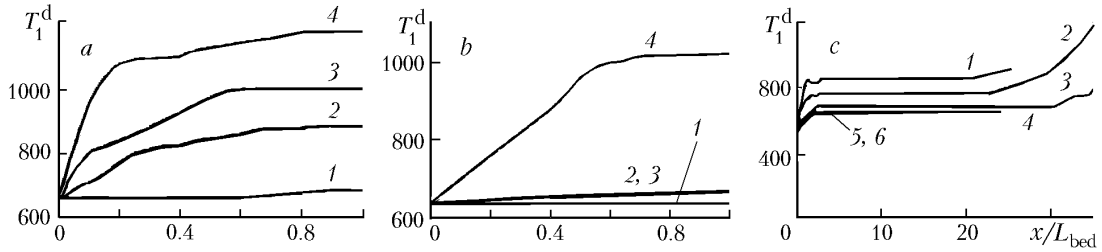

Fig. 1. Temperature profiles of the gas in the dense phase at different instants of time (a, b) and dynamics of change in the mass average temperature of the dense phase (c) as a function of pressure: a) $P_{0,1}$ = 0.1 MPa: 1) t = 0.01 sec, 2) 0.164, 3) 1.27, 4) 23.2; b) $P_{0,1}$ = 2.5 MPa: 1) t = 0.01 sec, 2) 0.164, 3) 14.9, 4) 88.2; c) $P_{0,1}$ = 0.1 MPa; 2) 0.25, 3) 0.55, 4) 0.868, 5) 1,65, 6) 2.5.

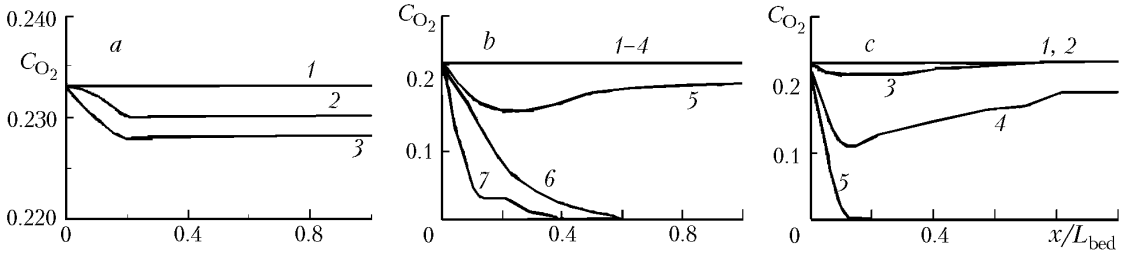

Fig. 2. Profiles of O_2 concentrations in the dense phase at different instants of time at $P_{0,1}$ = 0.1 MPa (a), 0.868 (b) and 2.5 (c): a) 1) $t = 0.2 \cdot 10^{-4}$ sec, $0.14 \cdot 10^{-3}$, $0.126 \cdot 10^{-2}$, $0.102 \cdot 10^{-1}$; 2) 0.164; 3) 1.27 and 12.6; b) 1–4) $t = 0.2 \cdot 10^{-4}$ sec, $0.14 \cdot 10^{-3}$, $0.126 \cdot 10^{-2}$, $0.102 \cdot 10^{-1}$, 5) 0.164, 6) 12.7, 7) 15.2; c) 1) $t = 0.2 \cdot 10^{-4}$ sec, 2) $0.14 \cdot 10^{-3}$, 3) $0.126 \cdot 10^{-2}$, 4) $0.102 \cdot 10^{-1}$, 5) 0.164.

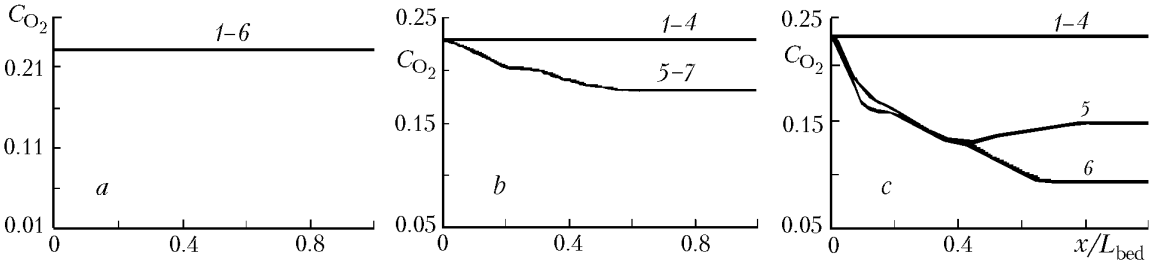

Fig. 3. Profiles of O_2 concentrations in the bubble phase at different instants of time at $P_{0,1}$ = 0.1 MPa (a), 0.868 (b), and 2.5 (c): a) 1) $t = 0.2 \cdot 10^{-4}$ sec, 2) $0.14 \cdot 10^{-3}$, 3) $0.126 \cdot 10^{-2}$, 4) $0.102 \cdot 10^{-1}$, 5) 0.164, 6) 1.27; b) 1) $t = 0.2 \cdot 10^{-4}$ sec, 2) $0.14 \cdot 10^{-3}$, 3) $0.126 \cdot 10^{-2}$, 4) $0.102 \cdot 10^{-1}$, 5) 0.164, 6) 1.51, 7) 15.2; c) 1) $t = 0.2 \cdot 10^{-4}$ sec, 2) $0.14 \cdot 10^{-3}$, 3) $0.126 \cdot 10^{-2}$, 4) 0.164, 5) 1.47, 6) 14.9.

flow of air and coal consumption, and the coefficients of heat and mass transfer between solid particles of coal and ash with a gas flow in the dense phase.

The results of the calculations confirmed the conclusions of [1–4] that despite the expansion of the stoichiometric mechanism of chemical reactions in the bed, the proposed mathematical model, computational algorithm, and program are fairly effective and stable and make it possible to attain, in the course of calculations, effective times of thermochemical transformation of the fuel comparable to those observed in pilot and pilot-production plants with different modifications of the fluidized bed.

Figures 1 and 2 present the results of the calculations for the influence of pressure on the gas temperature and the O_2 concentration in the dense phase. It is seen that, in general, the current characteristics of the process (profiles),

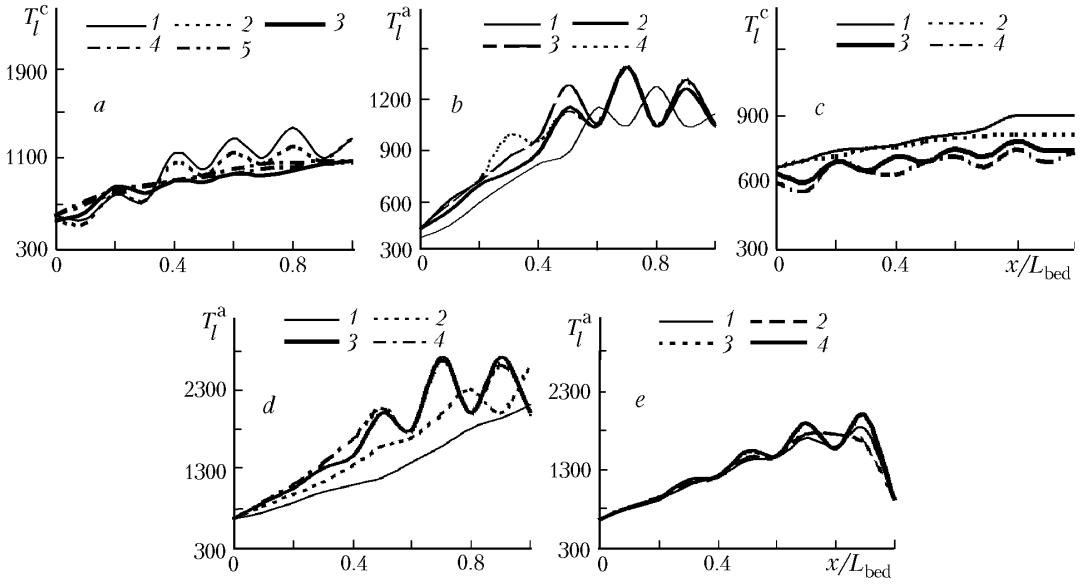

Fig. 4. Temperature profiles of different coke (a, c) and ash (b, d, e) fractions at the moment of the appearance of "hot" spots: a, b) $P_{0,1}$ = 0.1 MPa, t = 23.1 sec; c, d) 0.868 and 46.5; e) 2.5 MPa; 1) r_0^{sort} = 2.5 mm; 2) 2.05; 3) 1.3; 4) 0.8; 5) (0.5–0.1).

intensity with increasing pressure, and the mass-average temperature of the dense phase decreases somewhat, which is due to the retardation of the process by the gaseous components as a consequence of the reactions of gasification of the coke-ash residue of the fuel with CO_2 and H_2O.

Figure 3 shows the concentration profiles of oxygen in the dense phase on the bed height at various instants of time depending on the pressure. The results point to the intensification of the combustion process with increasing pressure.

The results of the calculations also confirmed the conclusions of [1–4] about the possible existence in the bed of so-called "hot spots" (short-time local heatings), in which the maximum temperature can be close to the temperature of the onset of fuel slagging (for which we took the temperature of onset of GSSh coal slagging close to 1400°C [32]) or even exceed it. This is evidenced by the temperature profiles of the coke and ash fractions at the moment of achieving "hot spots" for various pressures (Fig. 4). It can be seen that in the presence of additional combustible components in the bed, "hot spots" appear mainly at the upper points of the bed. The main reason for their appearance, as in [1–4], is the disturbance at the above points of the heat balance between the heat release as a result of the chemical transformations and the supply of heat from the environment due to convective and radiative heat transfer. However, this conclusion has to be refined by means of additional studies of the thermal stability of the process under consideration with regard for the possible effects of ash melting as in [33–35]. Such studies will be made in our further works.

The most stable calculations of the process were noted in calculating the heat and mass transfer coefficients by criterial relations [25].

CONCLUSIONS

1. We have developed a mathematical model, an algorithm, and a program for calculating the process of combustion–gasification of the multifractional coke residue of high-ash coal under pressure in a low-temperature fluidized bed at an expanded mechanism of homogeneous and heterogeneous chemical transformations.

2. It has been shown that despite the expansion of the mechanism of chemical reactions in the bed, the proposed mathematical model and computing algorithm and program are fairly effective and stable and permit a numerical analysis of the considered class of processes proceeding in a fluidized bed in a wide range of regime parameters of

functioning of apparatuses, their physical sizes, and physicochemical and structural characteristics of the fuel, attaining therewith effective times of fuel transformation comparable to those observed in pilot and pilot-production plants with different modifications of the fluidized bed. They also make it possible to test different hypotheses advanced, estimate parameters that are difficult to measure in experiments (observed rates of chemical transformations in the bed, interphase heat and mass transfer coefficients, effective coefficients of longitudinal transfer, etc.), predict optimal operational conditions of apparatuses, and search for regimes of slagless operation of the bed.

3. The investigations have confirmed the previously obtained numerical results on the possible existence in the bed of "hot spots" (short-time local heatings) in which the maximum temperature can be close to the temperature of onset of fuel slagging or exceed it and the possible mechanism of their appearance. The proceeding in the bed of additional heterogeneous and homogeneous chemical transformations intensifies the appearance of "hot spots" and promotes their displacement to the upper points of the bed.

4. It is preferable to use for numerical calculations criterial relations for the heat and mass transfer coefficients [25] taking into account the broader relationships between the sizes of the active fuel and inert ash particles in the bed than in [16].

NOTATION

$Ar^{sort} = [g(d_{part}^{eqv})^3(\rho_2^{sort} - \rho_{0,1})]/(\eta_1^2\rho_{0,1})$, Archimedes criterion; a, thermal diffusivity, $m^2 \cdot sec^{-1}$; C, concentration, mass fractions; $c_{p1}^{eff} = (c_{p1}\varepsilon_{mf}\rho_{0,1} + c_{p2}^{a}(1 - \varepsilon_{mf})\rho_2^{a})/(\varepsilon_{mf}\rho_{0,1} + (1 - \varepsilon_{mf})\rho_2^{a})$, effective heat capacity of the environment; c_p, specific heat capacity at a constant pressure, J/(kg·K); d, diameter, m; D, diffusion coefficient, m^2/sec; E, activation energy, J/mole; F, contour surface of particles, m^2/m^3; f, size distribution function of particles, m^{-1}; G, mass flow; $kg/(m^2 \cdot sec)$; g, acceleration of gravity, m/sec^2; K, carry-over rate constant, sec^{-1}; k^0, reference reaction rate constant at the initial gas or particle temperature, m/sec, $m^3/(kg \cdot sec)$ (for combustion and homogeneous reactions), MPa/sec, MPa^{-1} (for gasification reactions); L, bed height, m; m_{gas}, total number of gaseous components; M, molecular mass, kg/kmole; n_q and n_s, total number of homogeneous and heterogeneous reactions; N, total number of fractions of solid particles; $Nu = H_{conv}d_{part}^{eqv}/\lambda_1^{eff}$, Nusselt criterion; P, total pressure, Pa; p, partial pressures of reacting components, MPa; $Pr_1 = c_{p1}^{eff}\mu_1/\lambda_1^{eff}$, Prandtl criterion; Q, thermal effect of a reaction, J/kg; R, universal gas constant, J/(mole·K); r, particle radius, m; $Re = u_{mf}d_{part}^{eqv}\rho_{0,1}/\mu_1$, Reynolds criterion; $Sh_j = \beta_j d_{part}^{eqv}/D_{1j}$, Sherwood criterion; $Sc_1 = \eta_1/D_{1j}$, Schmidt criterion; t, time, sec; T, temperature, K; $\overline{T}^{*}$, averaged ambient temperature, K; u, speed of filtration of the gas in the bed, m/sec; u_0, feed rate of fuel under the bed, m/sec; x, coordinate of the bed height, m; y_k, molar fraction of CO (for reaction (8)) and CO_2 (for reaction (9)) (see (36)); W, reaction rate, $kg/(m^3 \cdot sec)$; α, volume fraction of bubbles in the bed; β, mass transfer coefficient between the gas flow in the dense phase of the bed and the particle surface, m/sec; γ, observed order of combustion reactions; δ, thickness of reactor walls, m; ε, porosity; $H_{b.e}$, coefficient of "dense phase–bubbles" interphase heat transfer, $W/(m^2 \cdot sec)$; $H_{b.c}$, coefficient of "gas circulation region–bubbles" heat transfer, $W/(m^2 \cdot sec)$; $H_{c.e}$, coefficient of heat transfer "gas circulation region–dense phase", $W/(m^2 \cdot sec)$; H_{conv}^{i}, heat transfer coefficient between the gas flow and the surface of particles, $W/(m^2 \cdot sec)$; H_w, flow-wall heat transfer coefficient, $W/(m^2 \cdot sec)$; η, kinematic viscosity, m^2/sec; κ, emissivity factor; $K_{b.e}$, coefficient of "dense phase–bubbles" interphase mass transfer, sec^{-1}; $K_{b.c}$, coefficients of "gas circulation region–bubbles" mass transfer, sec^{-1}; $K_{c.e}$, coefficient of heat and mass transfer "gas circulation region–dense phase", sec^{-1}; λ, heat conductivity coefficient, $W/(m^2 \cdot K)$; $\lambda_1^{eff} = \lambda_1\varepsilon_{mf} + \lambda_2^{a}(1 - \varepsilon_{mf})$, effective heat conductivity of the environment, $W/(m^2 \cdot K)$; μ, dynamic viscosity, Pa·sec; ν, stoichiometric coefficients; $\theta = E_q/RT_{0,1}$, $\theta_n = Q_q/RT_{0,1}$; ρ, density, kg/m^3; σ_0, Boltzmann, constant, $W/(m^2 \cdot K^4)$; $\upsilon = 1$ (for reaction (8)) and $\upsilon = 2$ (for reaction (9)) (see (36)); φ, fraction of the irradiated surface of particles; χ, generalized stoichiometric coefficient reflecting the proceeding of reactions of combustion of coals and cokes to CO or CO_2; ξ, particle shape factor; ψ, fractional portion of particles in the initial size distribution, m^{-1}; Ψ, bed mass, kg. Superscripts: d, dense phase; c, coke-ash residue; b, bubble phase; a, fraction of ash; p, pyroliser; sort, sort of particles (sort = c, coke; a, ash); surf, surface of a fuel particle; i, kind of the phase of the bed; eff, effective value; eqv, equivalent value; F, fixed value under normal conditions. Subscripts: 1, gas phase; j, gaseous component number; 1, CO_2; 2, CO; 3, H_2O; 4, H_2; 5, O_2; 6, CH_4; 7, N_2; sp, specific; s, heterogeneous reaction number; q, homogeneous reaction number; s,j, heterogeneous reaction, jth component; q,j, homogeneous reaction, jth component; 0,1, initial value, gas phase; 0,2, initial value, solid phase; l, solid fraction

number; ap, apparatus; b, bubbles; hov, hovering conditions; f, fuel; mf, conditions for the beginning of fluidizaction; cr, critical value; w, wall; b.c, circulation region–bubbles; c.e, circulation region–emulsion (dense) phase; b.e, bubbles–emulsion (dense) phase region; gas, gaseous; bed, bed; conv, convective; *, conditions for emersion of bubbles; car, carry-over; part, particle; 0, initial value; max, maximal; $\bar{}$, averaging.

REFERENCES

1. V. P. Patskov, N. V. Chernyavskii, and G. F. Kuznetsov, Mathematical simulation of nonstationary regimes of the processes of combustion and gasification of solid fuels in a low-temperature fluidized bed, in: *Solid-Fuel Power Technologies*, Ext. Abstr. of Papers presented at the scientific-technical meeting *"Problems of Energy Conversion and Use of Organic Fuel in Power Engineering"* [in Russian], Kiev (1992), pp. 2–3.
2. V. P. Patskov, Yu. P. Korchevoi, and A. Yu. Maistrenko, Numerical simulation of the process of combustion–gasification of high-ash pit coal in a pressurized fluidized bed, in: *Proc. 11th Int. Symposium "Chemical Physics of the Processes of Combustion and Explosion"* [in Russian], Vol. 1, Pt. 1, Chernogolovka (1996), pp. 135–140.
3. V. P. Patskov, Numerical simulation of the process of combustion–gasification of high-ash pit coal in a pressurized fluidized bed, *Visn. Ukr. Budin. Ekonom. Nauk.-Tekh. Zn.*, No. 8, 71–73 (1998).
4. O. Yu. Maistrenko, V. P. Patskov, O. I. Topal, Numerical analysis of the process of "wet" gasification of high-ash pit coal in a fluidized bed at elevated pressures, *Énergetika Élektrifikatsiya*, No. 5, 2–6 (2004).
5. V. P. Patskov, Numerical simulation of the process of thermochemical conversion of high-ash pit coal under pressure in a low-temperature fluidized bed, *Fiz. Goreniya Vzryva*, **38**, No. 2, 11–20 (2002).
6. É. P. Volkov, M. N. Egai, and R. Yu. Shakaryan, Mathematical model of coal combustion in a furnace with a fluidized bed, *Inzh.-Fiz. Zh.*, **52**, No. 6, 956–965 (1987).
7. É. P. Volkov, M. N. Egai, and R. Yu. Shakaryan, System-structural analysis of the physicochemical processes in a fluidized-bed furnace, in: *Use of Fuel and Environmental Protection*, Coll. Papers of the Moscow Power Engineering Institute, Moscow (1985), pp. 5–21.
8. Yu. P. Korchevoi and A. Yu. Maistrenko, Ecologically clean technologies of fluidized-bed combustion and gasification of coals, *Ékotekhnologii Resursosberezhenie*, No. 5, 3–10 (2001).
9. O. Yu. Maistrenko, *Basic Laws Governing Combustion and Gasification of High-Ash Coal in Various Modifications of the Fluidized Bed*, Author's Abstract of Doctoral Dissertation (in Engineering), Kiev (1999).
10. K. E. Makhorin and P. A. Khinkis, *Fluidized-Bed Combustion of Fuel* [in Russian], Naukova Dumka, Kiev (1989).
11. O. M. Todes and O. B. Tsitovich, *Apparatuses with a Granular Fluidized Bed. Hydraulic and Thermal Principles of Operation* [in Russian], Khimiya, Leningrad (1981).
12. V. V. Pomerantsev, K. M. Aref'ev, O. B. Akhmedov, et al., *Principles of the Practical Theory of Combustion* [in Russian], Énergoatomizdat, Leningrad (1986).
13. S. G. Ruzhnikov, O. V. Yangolov, M. L. Shchipko, and S. L. Gritsko, Modeling and optimization of the starting conditions of a fluidized-bed boiler, *Inzh.-Fiz. Zh.*, **59**, No. 1, 126–131 (1990).
14. D. Kunin and O. Levenspied, *Industrial Fluidization* [in Russian], Khimiya, Moscow (1976).
15. M. Radovanovich, *Fluidized-Bed Combustion of Fuel* [in Russian], Énergoatomizdat, Moscow (1990).
16. A. P. Baskakov, B. L. Lukachevskii, I. A. Mukhlenov, et al., in: I. P. Mukhlenov, B. S. Sazhin, and V. V. Frolov (Eds.), *Calculations of Fluidized-Bed Apparatuses: Handbook* [in Russian], Khimiya, Leningrad (1986).
17. V. P. Patskov, Mathematical treatment of experimental data on the kinetics of gasification of high-ash pit coal with CO_2 at elevated pressures, *Khim. Tverd. Topl.*, No. 4, 66–80 (2004).
18. N. M. Laurendeau, Heterogeneous kinetics of coal char gasification and combustion, *Progr. Energy Combust. Sci.*, **21**, No. 4, 221–270 (1978).
19. E. D. Scinner and L. D. Smoot, Heterogeneous reaction of char and carbon, in: L. D. Smoot and D. T. Pratt (Eds.) *Pulverized Coal Combustion and Gasification*, Plenum Press, New York–London (1979), pp. 160–167.
20. V. I. Bykov, T. I. Vishnevskaya, and N. M. Tsyryul'nichenko, Diffusion-kinetic model of combustion of coal particles in a gas flow, *Fiz. Goreniya Vzryva*, **33**, No. 4, 39–45 (1997).

21. A. W. Weimer and D. E. Glough, Modelling of low-pressure steam–oxygen gasification in fluidized bed coal gasifying reactor, *Chem. Eng. Sci.*, **36**, No. 3, 549–557 (1981).
22. S. Wegel and D. Luss, Steady-state multiplicity features of an adiabatic fixed-bed reactor with Langmuir–Hinshelwood kinetics: CO and CO_2 methanation, *Ind. Eng. Chem. Fundam.*, **23**, No. 2, 280–288 (1984).
23. T. V. Vilenskii and D. M. Khzmalyan, *Dynamics of Combustion of Dust-Like Fuel* [in Russian], Énergiya, Moscow (1978).
24. S. D. Beskov, *Technochemical Calculations* [in Russian], Vysshaya Shkola, Moscow (1966).
25. G. I. Pal'chenok, G. G. Vasil'ev, A. F. Dolidovich, et al., Heat- and mass transfer coefficients of an active particle freely moving in a fluidized bed of an inert disperse material, in: *Heat- and Mass Transfer–MIF-92*, *Proc. 2nd Minsk Int. Forum* [in Russian], 20–24 May 1992, Minsk (1992), Vol. 5, pp. 172–175.
26. J. G. Yates, *Fundamentals of Fluidized-Bed Chemical Processes* [Russian translation], Mir, Moscow (1986).
27. M. N. Shemyakin, V. N. Orlik, and K. I. Mishina, Mathematical simulation of the process of combustion and gasification of coal in a fluidized bed, *Khim. Tverd. Topl.*, No. 4, 128–133 (1988).
28. M. G. Slin'ko, V. S. Beskov, V. B. Skomorokhov, et al., in: A. Ermakov (Ed.), *Methods of Modeling Catalytic Processes on Analog and Digital Computers* [in Russian], Nauka, Novosibirsk (1972).
29. G. I. Marchuk, *Methods of Computational Mathematics* [in Russian], Nauka, Moscow (1980).
30. V. P. D'yakonov, *Handbook on Algorithms and Programs in the Basic Language for Personal Computers* [in Russian], Statistika, Moscow (1976).
31. M. Metcalf and J. Reed, *Programming Language FORTRAN-90* [Russian translation], Mir, Moscow (1995).
32. V. N. Yurenev and P. D. Lebedev (Eds.), *Heat Engineering Handbook* [in Russian], Énergiya, Moscow (1976).
33. I. S. Borisov, A. I. Bushma, and I. V. Krivtsun, Modeling of the motion and heating of powder particles in laser, flame, and hybrid spraying, *Dopov. NAN Ukrainy*, No. 1, 81–90 (2005).
34. V. G. Prokof'ev and V. K. Smolyakov, Nonstationary regimes of combustion of gas-free systems, *Fiz. Goreniya Vzryva*, **38**, No. 2, 21–25 (2002).
35. V. K. Smolyakov and D. S. Lapshin, Formation of the macroscopic structure of gas-free systems in the regime of force SHS-compaction, *Fiz. Goreniya Vzryva*, **38**, No. 2, 26–35 (2002).